A Projector Augmented Wave (PAW) code
for electronic structure calculations, Part I:
atompaw for generating atom-centered functions

N.A.W. Holzwarth [a,*], A.R. Tackett [b], G.E. Matthews [a]

[a] *Department of Physics, Wake Forest University, Winston-Salem, NC 27109, USA*
[b] *Department of Physics and Astronomy, Vanderbilt University, Nashville, TN 37235, USA*

Abstract

The computer program *atompaw* generates projector and basis functions which are needed for performing electronic structure calculations based on the Projector Augmented Wave (PAW) method. The program is applicable to materials throughout the periodic table. For each element, the user inputs the atomic number, the electronic configuration, a choice of basis functions, and an augmentation radius. The program produces an output file containing the projector and basis functions and the corresponding matrix elements in a form which can be read be the *pwpaw* PAW code. Additional data files are also produced which can be used to help evaluate the accuracy and efficiency of the generated functions. © 2001 Elsevier Science B.V. All rights reserved.

PROGRAM SUMMARY

Title of program: genproj

Catalogue identifier: ADNQ

Program Summary URL: http://cpc.cs.qub.ac.uk/summaries/ADNQ

Program obtainable from: CPC Program Library, Queen's University of Belfast, N. Ireland

Computers on which code has been tested: DEC Alpha, IBM SP2

Operating systems under which the program has been tested: Unix

Programming language used: Fortran90

Memory required to execute with typical data: 20 Mbytes or less

No. of bytes in distributed program, including test data, etc.: 1 173 014

Distribution format: gzip tar file

Nature of physical problem
The projector augmented wave (PAW) method, developed by Blöchl, is a very powerful tool for performing electronic structure

---

* Corresponding author.

E-mail addresses: natalie@wfu.edu (N.A.W. Holzwarth), alan.tackett@vanderbilt.edu (A.R. Tackett).

calculations within density functional theory, combining some of the best features of pseudopotential and all-electron approaches. Developing a procedure for constructing the projector and basis functions for a PAW calculations is similar to the challenge of constructing of pseudopotentials for a pseudopotential calculation. The construction scheme used in the present scheme is very similar to the one originally suggested by Blöchl and has now been demonstrated to work well for a number of complex materials.

Method of solution
The method starts with a self-consistent all-electron atomic structure calculation within the framework of density functional theory. The projector and basis functions are derived from the eigenstates of the all-electron atomic Hamiltonian. They are determined by iteratively solving radial differential equations.

Restrictions on the complexity of the program
All atoms in the periodic table can be treated with this approach, although those with high atomic numbers will have systematic errors due to the neglect of relativistic effects in this version of the code. The local density approximation (LDA) is coded for the exchange-correlation functional in this version of the code; other functionals, such as the generalized gradient approximation could easily be added.

Also, in this version of the code, it is assumed that electron density due to frozen core electrons is contained within the augmentation sphere. This assumption obviates the need for pseudo core wave functions or core tail density functions. The accuracy of this assumption can by controlled by including upper core states within the PAW basis set.

Typical running time
10 minutes or less.

Unusual features of the program
Some scripts are included to make it easy to generate plots of the output results using the Unix package *gnuplot*.

LONG WRITE-UP

1. Introduction

Since the introduction of the notion of the "norm-conserving" pseudopotential by Hamann, Schlüter, and Chiang [1] and Kerker [2], efforts have been made to perfect the physical and numerical accuracy of the pseudopotential formalism. While a table of pseudopotentials for all of the elements in the periodic table developed by Bachelet, Hamann, and Schlüter [3] has been well-used, many workers have instead developed modified functional forms, such as the generalized pseudopotential form of Hamann [4] and Blöchl [5], the plane-wave optimized form of Troullier and Martins [6], or the soft-pseudopotential form of Vanderbilt [7], which can be optimized for a particular material and computational technique. The computer code for generating pseudopotentials for elements throughout the periodic table, recently released by Fuchs and Scheffler [8], implements many of the ideas that have helped the development of the pseudopotential techniques during the past 20 years.

The Projector Augmented Wave (PAW) approach developed by Blöchl [9] goes beyond the pseudopotential approach and retains information about the all-electron calculation without significant additional computation. The problem of constructing the projector and basis functions needed for the PAW technique is very similar to the problem of constructing local and non-local pseudopotentials. In addition to Blöchl's original construction procedure, several others [10–12] have been suggested. The *atompaw* code uses a procedure similar to that originally suggested by Blöchl. It generates an output that is used by the *pwpaw* [13] code and additional outputs that allow the user to assess the accuracy and efficiency of the generated functions.

In this paper, we briefly present the formalism in Section 2.1 and show several examples which illustrate the choice of parameters in Section 2.2. A description of the *atompaw* and related programs is given in Section 3. A description of the input and output for *atompaw* is given in Section 4. Section 5 contains a few concluding remarks.

2. PAW basis and projector functions

2.1. Formalism

PAW calculations require a set of basis and projector functions which are denoted (in the notation of previous work [9–12]) $|\phi_i^a(\mathbf{r})\rangle$, $|\tilde{\phi}_i^a(\mathbf{r})\rangle$, and $|\tilde{p}_i^a(\mathbf{r})\rangle$, for the all-electron basis functions, pseudopotential basis functions, and projector functions, respectively. Here the "a" superscript denotes the atom index (which is suppressed in most of the remainder of this section), and the "i" subscript represents the atomic quantum numbers n_i, l_i, and m_i. Since these function are constructed from equations for a spherical atom, each can be written as a product of a radial function times a spherical harmonic function, such as:

$$\left|\phi_i^a(\mathbf{r})\right\rangle \equiv \left|\phi_{n_i l_i m_i}^a(\mathbf{r})\right\rangle \equiv \frac{\phi_{n_i l_i}^a(r)}{r} Y_{l_i m_i}(\hat{\mathbf{r}}). \tag{1}$$

The quantum number n_i is used to enumerate the radial functions $\phi_{n_i l_i}^a(r)$, $\tilde{\phi}_{n_i l_i}^a(r)$, and $\tilde{p}_{n_i l_i}^a(r)$ for a given angular momentum l_i. It often corresponds to the principal quantum number for the state but also can enumerate generalized functions needed for the basis [9]. Although the PAW method works using any of a variety of basis and projector functions, the efficiency and accuracy of the calculation are affected by this choice. In earlier work [10,11] we investigated several alternative construction schemes. However, we found a slight modification of the original scheme developed by Blöchl [9], to be the most robust.

The starting point of the construction process is an all-electron self-consistent solution of the Schrödinger equation for the reference atom or ion. It is assumed that the total electron density can be partitioned into a core electron density $n_{\text{core}}(r)$, corresponding to Q_{core} electrons and a valence electron density $n(r)$. The core density $n_{\text{core}}(r)$ is assumed to be fixed ("frozen") in the same form in the atom as it is in the solid. Thus, all of the calculational effort can be focused on the valence electrons. For some materials, especially transition metals or ionic compounds, it is prudent to extend the notion of "valence" electrons beyond the chemical definition to include upper core states. It is for the purpose of representing these generalized valence electrons in the atom and in the solid that we construct the basis and projector functions.

The all-electron basis functions $|\phi_i^0(\mathbf{r})\rangle$ are valence and continuum eigenstates of the Kohn–Sham [14] Hamiltonian. Here the superscript "0" is used to distinguish these initial basis functions from the final orthogonalized ones.

$$H(\mathbf{r})\left|\phi_i^0(\mathbf{r})\right\rangle = \varepsilon_i \left|\phi_i^0(\mathbf{r})\right\rangle, \tag{2}$$

The Hamiltonian is given in terms of the self-consistent valence density $n(r)$ by:

$$H(\mathbf{r}) = -\frac{\hbar^2}{2m}\nabla^2 + v_{\text{eff}}(r), \quad \text{where}$$
$$v_{\text{eff}}(r) \equiv v_{\text{ion}}(r) + e^2 \int d^3r' \frac{n(r')}{|\mathbf{r} - \mathbf{r}'|} + \mu_{\text{xc}}\big[n_{\text{core}}(r) + n(r)\big]. \tag{3}$$

Here $v_{\text{ion}}(r)$ denotes the ionic Coulomb potential

$$v_{\text{ion}}(r) = \frac{-Ze^2}{r} + e^2 \int d^3r' \frac{n_{\text{core}}(r')}{|\mathbf{r} - \mathbf{r}'|}, \tag{4}$$

with Z denoting the nuclear charge. The function μ_{xc} denotes the exchange correlation functional. In the present work, we used the local density approximation (LDA) form of Perdew and Wang [15], but other forms can be easily added to the code. Self-consistency implies that the valence density and the valence basis functions are related according to:

$$n(r) = \sum_{n_i l_i} w_{n_i l_i} \frac{|\phi_{n_i l_i}^0(r)|^2}{4\pi r^2}, \tag{5}$$

where $w_{n_i l_i}$ denotes the occupancy of the orbital "$n_i l_i$" which can be zero, especially for generalized functions.

The second consideration in constructing the basis and projector functions is to choose an appropriate augmentation radius r_c. This radius should be small enough so that for all the materials to be studied with these functions, the enclosing spheres do not overlap. On the other hand, it should be large enough so that core density $n_{\text{core}}(r)$ is well contained within r_c. [1]

In Blöchl's pseudo-function construction scheme, the smoothness of the functions is controlled by a shape function $k(r)$ which vanishes outside the augmentation region. Some possible choices of shape functions are:

$$k(r) = e^{-(r/\sigma)^{\lambda}} \quad \text{or} \quad k(r) = \begin{cases} \left[\dfrac{\sin(\pi r/r_c)}{(\pi r/r_c)} \right]^2 & \text{for } r < r_c, \\ 0 & \text{for } r \geqslant r_c, \end{cases} \tag{6}$$

where λ is typically 6. The squared sinc function form is generally found to have slightly better convergence properties in Fourier space than those of the exponential form.

The pseudo-basis functions $|\tilde{\phi}_i^0(\mathbf{r})\rangle$ are found by solving a self-consistent Schrödinger-like equation involving the "smooth" Hamiltonian $\widetilde{H}$. The equation takes the form:

$$\left(\widetilde{H}(\mathbf{r}) - \varepsilon_i \right) |\tilde{\phi}_i^0(\mathbf{r})\rangle = C_i k(r) |\tilde{\phi}_i^0(\mathbf{r})\rangle. \tag{7}$$

In this equation, ε_i is fixed at the all-electron eigenvalue found in Eq. (2), while C_i is to be determined. In numerically integrating the radial part of this equation for $\tilde{\phi}_{n_i l_i}^0(r)$, the coefficient C_i is adjusted so that $\tilde{\phi}_{n_i l_i}^0(r)$ has the correct number of nodes for each l value (zero nodes for the basis function with the lowest one-electron energy $\varepsilon_{n_i l_i}$, incremented by one node for each additional basis function at higher one-electron energies). In addition, the coefficient C_i is adjusted so that $\tilde{\phi}_{n_i l_i}^0(r)$ satisfies the boundary condition:

$$\tilde{\phi}_{n_i l_i}^0(r) = \phi_{n_i l_i}^0(r) \quad \text{for } r \geqslant r_c. \tag{8}$$

In practice, this is achieved by iterating Eq. (7) with variations in C_i so that the logarithmic derivatives of $\phi_{n_i l_i}^0(r_c)$ and $\tilde{\phi}_{n_i l_i}^0(r_c)$ are equal, following the approach described in Hartree's text [16]. The smooth Hamiltonian used in Eq. (7) is given by

$$\widetilde{H}(\mathbf{r}) = -\frac{\hbar^2}{2m} \nabla^2 + \tilde{v}_{\text{eff}}(r), \quad \text{where}$$
$$\tilde{v}_{\text{eff}}(r) \equiv \tilde{v}_{\text{loc}}(r) + e^2 \int d^3 r' \frac{\tilde{n}(r') + \hat{n}(r')}{|\mathbf{r} - \mathbf{r}'|} + \mu_{\text{xc}}\big[\tilde{n}(r)\big]. \tag{9}$$

In this expression for the smooth effective potential, the term $\tilde{v}_{\text{loc}}(r)$, denotes a local potential which vanishes outside the augmentation region. In the present work, this contribution is constructed in terms of the shape function:

$$\tilde{v}_{\text{loc}}(r) \equiv \mathcal{V}_0 k(r), \tag{10}$$

where $\mathcal{V}_0$ is a chosen amplitude. In our experience, most systems are not sensitive to this choice, however for highly ionic materials, the best choice for $\mathcal{V}_0$ seems to be the value which makes the non-local coefficient C_{i_s} in Eq. (7) vanish for the index i_s corresponding to the valence s-state of each material. An easy way to accomplish this, is to run the *atompaw* program once with $\mathcal{V}_0 = 0$ to determine the value of $C_{i_s}^0$ and then run the *atompaw* program a second time with $\mathcal{V}_0 = -C_{i_s}^0$. In fact, within numerical accuracy, the basis functions and projector functions are invariant to the choice of $\mathcal{V}_0$. From this point of view, we see that the role of $\mathcal{V}_0$ is to adjust the strength of the local potential contributions relative to the strength of the non-local contributions for each atom. [2]

---

[1] In the present version of the code we set the core tail function defined in Ref. [10] identically to zero since we find that whenever the core density has a contribution which is appreciable for $r > r_c$, it is a better approximation to represent those upper core electrons as generalized valence electrons.

[2] This procedure differs from that of Blöchl [9] who determines $\tilde{v}_{\text{loc}}(r)$ by unscreening a constructed pseudopotential.

At self-consistency, the pseudo-density $\tilde{n}(r)$ in Eq. (9) is determined from the pseudo-basis functions

$$\tilde{n}(r) = \sum_{n_i l_i} w_{n_i l_i} \frac{|\tilde{\phi}^0_{n_i l_i}(r)|^2}{4\pi r^2}. \tag{11}$$

The additional Coulombic contribution in Eq. (9) denoted by $\hat{n}(r)$, represents the compensation charge density which is needed to correct the total atomic charge. This charge density is spherically symmetric for the atom and can be written:

$$\hat{n}(r) = Q_{00} g_{00}(\mathbf{r}), \tag{12}$$

where the monopole moment Q_{00} is

$$Q_{00} \equiv -Z + Q_{\text{core}} + \int \mathrm{d}^3 r \big[n(r) - \tilde{n}(r) \big]. \tag{13}$$

The functional form of atom-centered moments of the compensation charge is now chosen to be proportional to the shape function:

$$g_{LM}(\mathbf{r}) \equiv \mathcal{N}_L r^L k(r) Y_{LM}(\hat{\mathbf{r}}), \quad \text{where}$$
$$\big[\sqrt{4\pi}\, \mathcal{N}_L \big]^{-1} \equiv \int\limits_0^{r_c} \mathrm{d}r\, r^{2+2L} k(r). \tag{14}$$

Here, $Y_{LM}(\hat{\mathbf{r}})$ denotes the spherical harmonic function and $\mathcal{N}_L$ denotes a normalization factor.

Once the pseudo-basis functions $|\tilde{\phi}^0_i\rangle(\mathbf{r})$ have been determined by self-consistently solving Eq. (7), the corresponding projector functions are formed according to:

$$\big|\tilde{p}^0_i(\mathbf{r})\big\rangle \equiv \frac{k(r)|\tilde{\phi}^0_i(\mathbf{r})\rangle}{\langle\tilde{\phi}^0_i|k|\tilde{\phi}^0_i\rangle}. \tag{15}$$

This means that these initial pseudo-basis functions and the corresponding projector functions are normalized according to

$$\langle\tilde{\phi}^0_i|\tilde{p}^0_i\rangle = 1, \tag{16}$$

and related to the smooth Hamiltonian according to the identity:

$$\big(\widetilde{H}(\mathbf{r}) - \varepsilon_i\big)\big|\tilde{\phi}^0_i(\mathbf{r})\big\rangle = \big|\tilde{p}^0_i(\mathbf{r})\big\rangle\big\langle\tilde{\phi}^0_i\big|\widetilde{H} - \varepsilon_i\big|\tilde{\phi}^0_i\big\rangle. \tag{17}$$

The final basis and projector functions $\{|\phi_i(\mathbf{r})\rangle, |\tilde{\phi}_i(\mathbf{r})\rangle, |\tilde{p}_i(\mathbf{r})\rangle\}$ are formed from the initial functions $\{|\phi^0_i(\mathbf{r})\rangle, |\tilde{\phi}^0_i(\mathbf{r})\rangle, |\tilde{p}^0_i(\mathbf{r})\rangle\}$ by a Gram–Schmidt orthogonalization procedure as described in Eqs. (91)–(96) of Ref. [9]. Specifically, for each angular momentum quantum number l, we denote the successive radial functions with indices $n_1, n_2, \ldots$, etc. The first set of basis and projector functions is given by the initial functions:

$$\tilde{p}_{n_1 l}(r) \equiv \tilde{p}^0_{n_1 l}(r), \quad \tilde{\phi}_{n_1 l}(r) \equiv \tilde{\phi}^0_{n_1 l}(r), \quad \text{and} \quad \phi_{n_1 l}(r) \equiv \phi^0_{n_1 l}(r). \tag{18}$$

If there is a second radial basis function for that l, the final function is orthonormalized with respect to the first according to:

$$\tilde{p}_{n_2 l}(r) = \mathcal{F}_{n_2 l}\big[\tilde{p}^0_{n_2 l}(r) - \tilde{p}_{n_1 l}(r)\langle\tilde{\phi}_{n_1 l}|\tilde{p}^0_{n_2 l}\rangle\big],$$
$$\tilde{\phi}_{n_2 l}(r) = \mathcal{F}_{n_2 l}\big[\tilde{\phi}^0_{n_2 l}(r) - \tilde{\phi}_{n_1 l}(r)\langle\tilde{p}_{n_1 l}|\tilde{\phi}^0_{n_2 l}\rangle\big], \tag{19}$$
$$\phi_{n_2 l}(r) = \mathcal{F}_{n_2 l}\big[\phi^0_{n_2 l}(r) - \phi_{n_1 l}(r)\langle\tilde{p}_{n_1 l}|\tilde{\phi}^0_{n_2 l}\rangle\big],$$

where

$$\mathcal{F}_{n_2 l} \equiv \left(1 - \langle \tilde{\phi}_{n_2 l}^0 | \tilde{p}_{n_1 l} \rangle \langle \tilde{\phi}_{n_1 l} | \tilde{p}_{n_2 l}^0 \rangle \right)^{-1/2}. \tag{20}$$

If there were additional radial basis functions for that l, they would be orthonormalized in a similar way. In our experience, and in that of previous workers [5,17], one or two radial basis functions are usually sufficient to span the Hilbert space of smooth functions within each atomic sphere.

In terms of these basis functions, the generalized eigenvalue equation for the PAW formalism can be written

$$\mathbf{H}^{\mathrm{PAW}}(\mathbf{r}) \big| \widetilde{\Psi}_E(\mathbf{r}) \big\rangle = E \mathbf{O} \big| \widetilde{\Psi}_E(\mathbf{r}) \big\rangle, \tag{21}$$

where

$$\mathbf{H}^{\mathrm{PAW}} \equiv \widetilde{H}(\mathbf{r}) + \sum_{aij} \big| \tilde{p}_i^a \big\rangle \big(\langle \phi_i^a | H^a | \phi_j^a \rangle - \langle \tilde{\phi}_i^a | \widetilde{H}^a | \tilde{\phi}_j^a \rangle \big) \big\langle \tilde{p}_j^a \big|, \tag{22}$$

and

$$\mathbf{O} \equiv \mathbf{1} + \sum_{aij} \big| \tilde{p}_i^a \big\rangle \big(\langle \phi_i^a | \phi_j^a \rangle - \langle \tilde{\phi}_i^a | \tilde{\phi}_j^a \rangle \big) \big\langle \tilde{p}_j^a \big|. \tag{23}$$

The eigenstates $|\widetilde{\Psi}_E(\mathbf{r})\rangle$ of Eq. (21) are related to the eigenstates of the all-electron Hamiltonian, according to:

$$\big| \Psi_E(\mathbf{r}) \big\rangle = \big| \widetilde{\Psi}_E(\mathbf{r}) \big\rangle + \sum_{ai} \big(|\phi_i^a(\mathbf{r})\rangle - |\tilde{\phi}_i^a(\mathbf{r})\rangle \big) \big\langle \tilde{p}_i^a \big| \widetilde{\Psi}_E \big\rangle, \tag{24}$$

within the accuracy of the PAW representation. For the case of a spherically symmetric atom, the site index a is trivial and all matrix elements are diagonal in $l_i m_i$ indices. By construction, the valence density $n(r)$ (Eq. (5)) and pseudo-density $\tilde{n}(r)$ (Eq. (11)) are expressed in terms of the initial $\phi_{n_i l_i}^0(r)$ and $\tilde{\phi}_{n_i l_i}^0(r)$ basis functions which determine the all-electron (2) and and smooth (9) Hamiltonians. In turn, these Hamiltonians are used to generate these functions and the projectors. It can be shown that, after the orthonormalization procedure of Eqs. (18), (19), and (20), the initial pseudo-wavefunctions $|\tilde{\phi}_i^0(\mathbf{r})\rangle$ are eigenstates of the atomic PAW Hamiltonian (21), with corresponding eigenvalues ε_i of the all-electron Hamiltonian (2). More generally, the Hamiltonians H^a and $\widetilde{H}^a$ which appear in Eq. (22) are defined in terms of matrix elements evaluated using the orthogonalized basis functions $\{\phi_i^a\}$ and $\{\tilde{\phi}_i^a\}$ [9,10,13]. The construction procedure ensures that $\mathbf{H}^{\mathrm{PAW}}$ reproduces the same eigenvalue spectrum as the all-electron Hamiltonian within the energy range spanned by the basis functions.

2.2. Examples

Fig. 1 shows an example of a set of projector and basis functions generated for Mo. These functions have been successfully used in the study of the electronic structure of $CaMoO_4$ and related materials [18]. In this example there are two projector and basis sets for each l value. For each l, the first $\tilde{\phi}_{nl}(r)$ and $\tilde{p}_{nl}(r)$ functions have no nodes, while the functions for the second set have one node.

In general, as in the construction of pseudopotentials [8], one often has to balance accuracy versus efficiency in order to generate the best basis and projector functions for a given material. Greater accuracy is achieved by choosing r_c to be small and faster convergence in the plane wave expansion is obtained by choosing r_c to be large. To quantify the plane wave convergence, we can define a Fourier-space function:

$$F_{n_i l_i}(q) \equiv \bar{\tilde{p}}_{n_i l_i}(q) \bar{\tilde{\phi}}_{n_i l_i}(q) q^2. \tag{25}$$

Here $\bar{\tilde{p}}_{n_i l_i}(q)$ and $\bar{\tilde{\phi}}_{n_i l_i}(q)$ represent the Fourier transforms of the radial functions $\tilde{p}_{n_i l_i}(r)$ and $\tilde{\phi}_{n_i l_i}(r)$, respectively. The integral of $F_{n_i l_i}(q)$ with respect to q is related, through Parseval's relation to the radial integral involved with calculating the overlap of a projector function with the corresponding pseudo-basis function. The
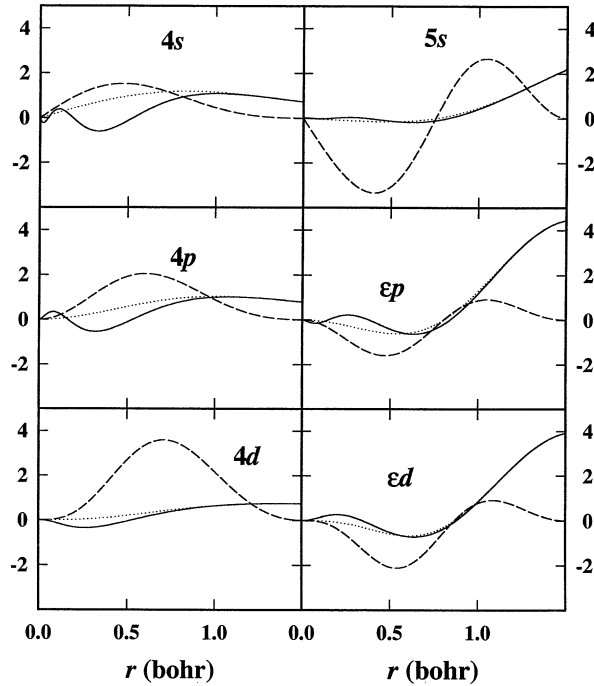
Fig. 1. Plot of radial projector and basis functions for Mo generated using the squared sinc form of the shape function and $r_c = 1.5$ bohr. For each nl, the $\phi_{nl}(r)$, $\tilde{\phi}_{nl}(r)$, and $\tilde{p}_{nl}(r)$ functions are plotted with solid, dottes, and dashed lines, respectively.

non-zero range of $F_{n_i l_i}(q)$ is a good indication of the plane wave convergence of the overlap integral $\langle \tilde{p}_i^a | \tilde{\Psi}_{n\mathbf{k}} \rangle$ of the projector function with a Bloch pseudo-wavefunction.

We illustrate the plane wave convergence for the $2p$ basis functions for O in Fig. 2 where the choices of $r_c = 1.0$ and 1.3 bohr and the effects of the exponential ("exp") and squared sinc ("sinc") functional forms for the shape function $k(r)$ are compared. The "exp" form was chosen with $\lambda = 6$ and $\sigma \approx 0.65 r_c$ (so that $k(r_c) \approx 1 \times 10^{-6}$). In Fig. 2 we see that the functions generated with $r_c = 1.3$ bohr converge much more rapidly that those generated with $r_c = 1.0$ bohr. We also see that the function formed using the exponential shape function has a small oscillation at large q, while the function formed with the squared sinc shape function goes smoothly to zero.

To further assess these choices, we have carried out calculations on the electronic structure of CaO using these functions with the *pwpaw* [13] code. For the purpose of this test, Ca projectors and basis functions where fixed. They were constructed with the "sinc" shape functions with $r_c = 1.5$ bohr, including $3s$, $4s$, $3p$, εp, and $3d$ functions.[3] Four different choices for the O projector and basis functions were studied including the exponential and squared sinc shape functions and $r_c = 1.4$ or 1.2 bohr as indicated in Table 1 and in the legends of Figs. 3, 4, and 5. In Fig. 3, we show a plot of the negative of the cohesive energy of CaO as a function of cubic lattice constant a. The calculated lattice constant results were fit to the Murnaghan equation of state [19]. The resulting fit values of the lattice parameter, bulk modulus, and cohesive energy are summarized in Table 1. It is reassuring to notice that these results are very insensitive to the choice of the projector and basis functions as they should be. The small variations in the equilibrium cohesive energies are due to differences in the solid and atomic calculations which

---

[3] In order to ensure that the second $l = 1$ radial basis functions for Ca are orthogonal to the $3p$ basis functions, it is convenient to choose a continuum basis function $\phi_{\varepsilon p}(r)$ which has 3 nodes well within the augmentation region in place of $\phi_{4p}(r)$ whose 3rd node is inconveniently close to the augmentation radius.
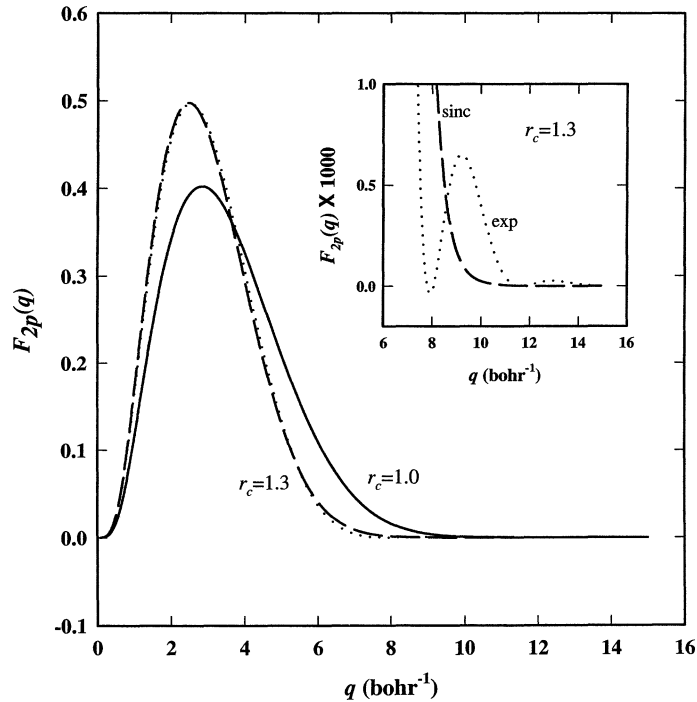
Fig. 2. Plot of $F_{2p}(q)$ defined in Eq. (25) for the $2p$ states of O plotted as a function of q, comparing results for $r_c = 1.0$ and $r_c = 1.3$ bohr. Insert compares results on an expanded scale using two forms for weight functions $k(r)$ as indicated.

Table 1
Comparison of the equilibrium fit parameters for CaO $- E_0$ (cohesive energy), B (bulk modulus), and a_0 (lattice constant) for 4 choices for projector and basis functions of O, corresponding to 4 curves plotted in Fig. 3

Label	$\{n_i l_i\}$	E_0 (eV/atom)	a_0 (Å)	B (GPA)
"exp", rc=1.4	$2s, 2p$	7.176	4.704	126
"sinc", rc=1.4	$2s, 2p$	7.174	4.705	126
"sinc", rc=1.2	$2s, 2p$	7.185	4.703	127
"sinc", rc=1.4 ($\times 2$)	$2s, \varepsilon s, 2p, \varepsilon p$	7.195	4.700	127

cancel each other slightly differently in each case. The equilibrium lattice constant varies by less that 0.1% and the bulk modulus by less than 1%.

On the other hand, the number of plane-waves needed to converge a calculation is more sensitive to these choices as seen in Fig. 4, where the negative of the cohesive energy is plotted versus the plane-wave cutoff parameter (labeled "Gcut_LOW" in correspondence with the notation used in the *pwpaw* code). Here we see that the sinc shape form converges more rapidly as a function of plane-wave cutoff than does the exponential shape form even when additional basis functions are added for $r_c = 1.4$ bohr. In fact, the sinc shape function with $r_c = 1.2$ bohr results converge at approximately the same plane-wave cutoff as those using the exponential shape function with $r_c = 1.4$ bohr for this example.

The accuracy of a calculation can also be sensitive to the choice of basis function. In Fig. 5 we show the calculated logarithmic derivatives for generalized $l = 1$ (p) radial functions of O for projector and basis functions
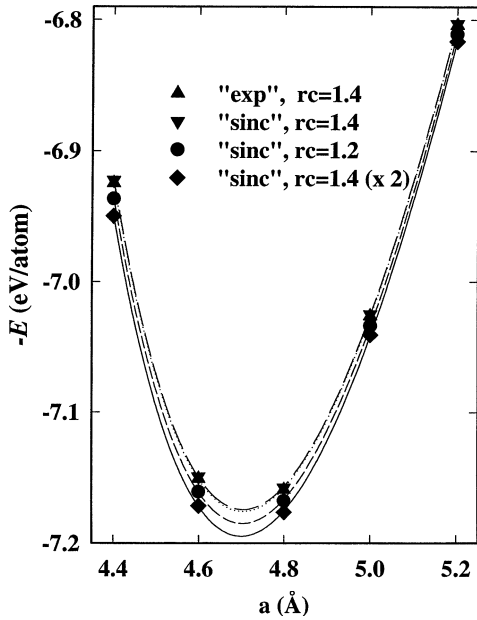
Fig. 3.
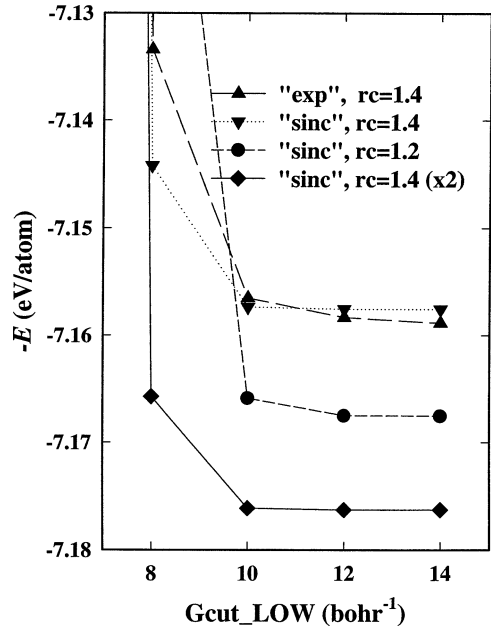
Fig. 4.

Fig. 3. Plot of the negative of the cohesive energy of CaO as a function of the cubic lattice parameter a. These results were obtained using the *pwpaw* code [13] with 4 different choices for the O basis and projector functions as indicated. The lines through the symbols represent fits to the Murnaghan equation of state [19].

Fig. 4. Plot of the negative of the cohesive of CaO at fixed lattice constant E ($a = 4.8$ Å) as shown in Fig. 3, showing the dependence on the plane wave convergence parameter Gcut_LOW for the 4 different choices for the O basis and projector functions.

Fig. 5. Plot of the logarithmic derivatives of the $l = 1$ (p) radial wavefunctions for O as a function of energy E. Results of all-electron 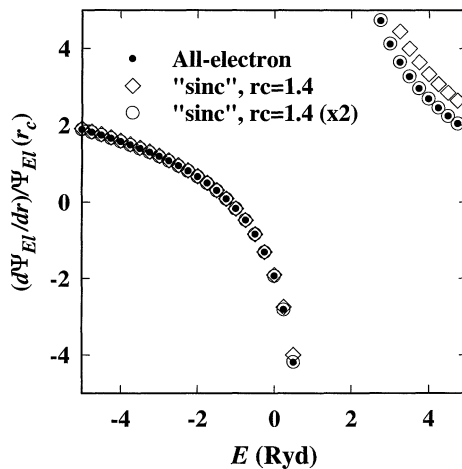wavefunctions are compared with wavefunctions obtained from solving the atomic PAW equation (21), comparing two different choices of projector and basis functions.

at $r_c = 1.4$ bohr. The results generated with a single basis function start to diverge from all-electron logarithmic derivatives for energies $E > 1$ Ryd. This is true for the exponential shape function (not plotted) as well as the squared sinc shape function shown in the plot. The use of a second $l = 1$ basis function brings the PAW result into agreement with the all-electron logarithmic derivatives for E values at least up to 5 Ryd. Apparently, as shown in Table 1, this behavior of the logarithmic derivatives at $E > 1$ Ryd. Does not appreciably effect the calculated equilibrium properties of CaO, however.

Another consideration in the choice of $\{r_c^a\}$ is the possibility of the appearance of "ghost" states which has been well-characterized by Gonze and co-workers [20,21] for separable Hamiltonians and also plagues other electronic structure methods [22]. For non-local pseudopotentials of the Kleinman–Bylander [23] form, guidelines have been developed by Gonze and co-workers [20,21] for avoiding these problems. These guidelines, could be applied to the PAW formalism, however, since both the local and non-local parts of the Hamiltonian are updated during the SCF cycle, for a given set of projector and basis functions, the appearance of ghost states can be material dependent. In our experience, reducing the $\{r_c^a\}$ values is an effective method of getting rid of ghost-state instabilities.

3. Description of the programs

3.1. atompaw

All data within the program are expressed in Rydberg atomic units unless otherwise stated. The program input is discussed in Section 4 below. In order to simplify the operation, some integration variables have been preset. Some of these may need to be tested for accuracy or adjusted for some compilers. For example, the numerical integrations are performed on a range of 50 bohr using 20 000 integration points and a convergence tolerance of 10^{-15}. On some compilers, we have had to increase the tolerance slightly. These parameters are set in the subroutine dfatom.f90. [4]

At the end of the calculation *atompaw* generates an output summary file, several diagnostic data files, and an atomic data file which is used by the *pwpaw* program. The atomic data file is named [atomic symbol].atomicdata and is organized as follows. The set of radial projector and basis functions $\tilde{p}_{n_i l_i}(r)$, $\phi_{n_i l_i}(r)$, $\tilde{\phi}_{n_i l_i}(r)$ are each tabulated on a uniform radial mesh $r = vh$, where $0 \leqslant v \leqslant (\text{MESH\_SIZE} - 1)$. Here the "MESH_STEP" parameter h is chosen so that $r_c = (\text{MESH\_SIZE} - 1)h$. The $\tilde{\phi}_{n_i l_i}(r)$ basis functions are also needed in a larger radial range for generating an initial guess of the eigenstates of the system. For this purpose, a second radial mesh is defined with the form $r = vh_{\text{LCAO}}$ with $0 \leqslant v \leqslant (\text{LCAO\_SIZE} - 1)$.

Single valued data are listed in the following form.

KEYWORD value

Table 2 enumerates these keywords and their meanings. The last entry is the total valence energy of the atom E_{atom}^a which is used to calculate the cohesive energy of a multi-atomic system.

Also in the [atomic symbol].atomicdata file, multiple value data are listed in the form:

KEYWORD Index
   list of values
END

The "Index" is necessary for some of the keywords, but not others. Table 3 summarizes these keywords for the multiple value data. The form of the matrix elements listed in the tables have been defined in earlier work with a

---

[4] In the current version of the code, a uniform radial mesh is used to represent all functions. This choice is ideal for processing all the smooth functions. By choosing a relatively fine mesh and by using high order integration algorithms, the uniform mesh can also work well for the all-electron functions. For example, the Numerov algorithm [24] is used to integrate the Schrödinger equation. The preset mesh size has been tested for elements through the 5th row of the periodic table. For heavier elements, the errors of neglecting the relativistic effects are probably comparable to integration errors.

Table 2
List of keywords for single value data in the [atomic symbol].atomicdata file. Examples are taken from calculation for O

Keyword	Example	Description
ATOMTYPE	O	atomic symbol
ATOMIC_CHARGE	8	Z^a
CORE_CHARGE	2.0	Q_{core}^a
RC	1.41	r_c^a
VLOC	0.0	$\mathcal{V}_0^a$
SHAPE_TYPE	sinc2	"sinc2" or "exshape"
MESH_SIZE	565	number of mesh points for $0 \leqslant r \leqslant r_c^a$
MESH_STEP	0.0025	h^a
LCAO_SIZE	642	number of LCAO mesh points
LCAO_STEP	0.0125	h_{LCAO}^a
BASIS_SIZE	4	total number of $n_i l_i$'s for atom a
OVERLAP_SIZE	6	number of $O_{n_i l_i n_j l_j}^a$ matrix elements
DENVHAT_SIZE	13	number of $n_{n_i l_i n_j l_j}^{aL}$ matrix elements
HARTREE_SIZE	73	number of $V_{n_i l_i n_j l_j; n_k l_k n_l l_l}^{aL}$ matrix elements
ENERGY	-31.70159	valence total energy of atom, E_{atom}^a
END		end of data set

Table 3
List of keywords for multiple value data in the [atom symbol].atomicdata file

Keyword	Index	Description
ORBITALS		l_i, $1 \leqslant i \leqslant$ BASIS_SIZE
TPROJECTOR	i	$\tilde{p}_{n_i l_i}^a(\nu h)$ (MESH_SIZE entries for each i)
TPHI	i	$\tilde{\phi}_{n_i l_i}^a(\nu h)$ (MESH_SIZE entries for each i)
PHI	i	$\phi_{n_i l_i}^a(\nu h)$ (MESH_SIZE entries for each i)
CORE_DENSITY		$n_{\text{core}}^a(\nu h)$ (MESH_SIZE entries)
SHAPE_FUNC		$k^a(\nu h)$ (MESH_SIZE entries)
LCAO_TPHI	i	$\tilde{\phi}_{n_i l_i}^a(\nu h_{\text{LCAO}}^a)$ (LCAO_SIZE entries for each i)
OVERLAP_MATRIX		$O_{n_i l_i n_j l_i}^a$ (OVERLAP_SIZE entries)
KINETIC_ENERGY_MATRIX		$K_{n_i l_i n_j l_i}^a$ (OVERLAP_SIZE entries)
V_ION_MATRIX		$[v_{\text{at}}]_{n_i l_i n_j l_i}^a$ (OVERLAP_SIZE entries)
DENSITY		$i\ j\ L\ n_{n_i l_i n_j l_j}^{aL}$ (DENVHAT_SIZE entries)
V_HAT		$i\ j\ L\ \hat{v}_{n_i l_i n_j l_j}^{aL}$ (DENVHAT_SIZE entries)
V_HARTREE		$i\ j\ k\ l\ L\ V_{n_i l_i n_j l_j; n_k l_k n_l l_l}^{aL}$ (HARTREE_SIZE entries)
HAT_SELF-ENERGY	L_{max}^a	$L\,\widehat{E}^{aL}$ ($L_{\text{max}}^a + 1$ entries)

Table 4
List of plotable output files for *atompaw*

File name	Data columns	Plotting script
wfn$i$	$r\ \phi^a_{n_i l_i}(r)\ \tilde{\phi}^a_{n_i l_i}(r)\ \tilde{p}^a_{n_i l_i}(r)$	plotwfn i $(i = 1, \ldots)$
wfnr$i$	$r\ \phi^a_{n_i l_i}(r)/r\ \tilde{\phi}^a_{n_i l_i}(r)/r\ \tilde{p}^a_{n_i l_i}(r)/r$	
density	$r\ n_{\mathrm{core}}(r)\ n(r)\ \tilde{n}(r)$	plotdensity
potential	$r\ v_{\mathrm{eff}}(r)\ \tilde{v}_{\mathrm{eff}}(r)$	plotpotential
logderiv.l	$E\ (\mathrm{d}\Psi_{El}/\mathrm{d}r)/\Psi_{El}(r_c)\ (\mathrm{d}\widetilde{\Psi}_{El}/\mathrm{d}r)/\widetilde{\Psi}_{El}(r_c)$	plotlogderiv l $(l = 0, \ldots)$
tprod.i	$q\ F_{n_i l_i}(q)$	
pj.i	$q\ \bar{\tilde{p}}_{n_i l_i}(q)$	
tphij.i	$q\ \bar{\tilde{\phi}}_{n_i l_i}(q)$	

few modifications described as follows. The matrix elements which are diagonal in the l_i and l_j quantum numbers, $O^a_{n_i l_i n_j l_i}$ and $K^a_{n_i l_i n_j l_i}$, are defined in [10, Eqs. (A9) and (A10)], respectively. The ionic and local potential matrix elements have been combined into a single term defined according to:

$$[v_{\mathrm{at}}]^a_{n_i l_i n_j l_i} \equiv \int\limits_0^{r_c^a} \mathrm{d}r \left(\phi^a_{n_i l_i}(r) v_{\mathrm{ion}}(r) \phi^a_{n_j l_i}(r) - \tilde{\phi}^a_{n_i l_i}(r) \tilde{v}_{\mathrm{loc}}(r) \tilde{\phi}^a_{n_j l_i}(r) \right). \tag{26}$$

The matrix elements which depend on a "total" angular momentum L, $n^{aL}_{n_i l_i n_j l_j}$, $\hat{v}^{aL}_{n_i l_i n_j l_j}$, and $V^{aL}_{n_i l_i n_j l_j; n_k l_k n_l l_l}$ are defined in [10, Eqs. (A13), (A16), and (A17)], respectively. Because of the new form of the moments of the compensation charge density (14), the Coulomb self-energy [10, Eq. (20)] can be determined by summing over contributions from the tabulated moments $\widehat{E}^{aL}$ defined by

$$\widehat{E}^{aL} \equiv \frac{1}{2} \int \mathrm{d}^3 r\, \mathrm{d}^3 r' \frac{g_{\mathrm{LM}}(\mathbf{r}) g_{\mathrm{LM}}(\mathbf{r}')}{|\mathbf{r} - \mathbf{r}'|}. \tag{27}$$

3.2. Gnuplot scripts for plotting output files

Several files are generated by *atompaw* which are designed to be used for diagnostic purposes. Table 4 lists their names, columnar data, and calling sequence for use of supplied script which is designed to be used with the Unix package *gnuplot*.

The Fourier transform results are unfortunately only useful for the bound-state basis functions, since the Fourier transforms of the continuum functions are, in principle, delta functions in wave vector, but are not properly calculated in the program.

4. Sample input and output

The program *atompaw* was designed to be run interactively. However, since it is often necessary to optimize the parameters, it is convenient to use an input file. Sample input files for some of the O examples are shown in Figs. 6 and 8, with the corresponding output summary files in Figs. 7 and 9, respectively. In addition to the summary file, the program generates a number of additional output files as described in Section 3.2. For each new material or parameter set, it is therefore desirable to run the program in an appropriately named subdirectory.

```
O                    Atom summary file name
8                    Z
2 2 0 0 0            maximum n for s, p, d, f, g shells
2 1 4               correction to maximum occupancy (n l occ)
0 0 0               end corrections
c                    core state
v                    valence state
v                    valence state
ipass                use default parameters
1                    lmax
1.4                  rc
y                    add new l=0 basis function
7                    energy for new l=0 basis function
n                    no new l=0 basis functions
y                    add new l=1 basis function
7                    energy for new l=1 basis function
n                    no new l=1 basis functions
O                    Atom symbol
c                    continue
2                    new valence occupancy
4                    new valence occupancy
c                    continue
2                    new valence occupancy
3                    new valence occupancy
e                    exit
```

Fig. 6. Input data for O projector and basis functions corresponding to "sinc", rc = 1.4 (×2) case.

The following shows a portion of an interactive run of the program for the case described above as "sinc" rc = 1.4 (×2). The lines beginning with ≫ denote input data and generates the same results as the input file shown in Fig. 6.

```
 enter energy output file name
>>O
 enter atomic number
>>8
 Calculation for atomic number = 8
 enter maximum principle quantum numbers for s,p,d,f,g
>>2 2 0 0 0
ns np nd nf ng = 2 2 0 0 0
 3 orbitals will be calculated
 Below are list the default occupations
 n l    occupancy
 1 0     2.000000E+00
 2 0     2.000000E+00
 2 1     6.000000E+00
  enter np l occ for all occupations for all revisions
   enter 0 0 0. to end
>>2 1 4
>>0 0 0
Corrected occupations are:
 n l    occupancy
 1 0     2.000000E+00
 2 0     2.000000E+00
 2 1     4.000000E+00
```

```
            nz =  8
            Integration params -- n,rmax,small = 20000  5.0000000E+01  1.0000000E-15
              all-electron results
              core states (zcore) =  1.99999999999999334
                 1    1    0  2.0000000E+00 -3.7516303E+01
              valence states (zvale) =  6.00000000000001332
                 2    2    0  2.0000000E+00 -1.7424442E+00
                 3    2    1  4.0000000E+00 -6.7652133E-01
             evale =  -31.7015931876238355
              paw parameters:
                 shapef = sinc2
                   lmax =  1
                     rc =  1.40999999999999992
                  iiirc =  564
                 vlocfac =  0.000000000000000000E+00
             Using Blochl method

            Number of basis functions      4
               No.   n   l      Energy        Cp coeff
                 1    2    0 -1.7424442E+00 -2.3987351E+00
                 2  999    0  7.0000000E+00 -7.1621022E+00
                 3    2    1 -6.7652133E-01  8.8537607E+00
                 4  999    1  7.0000000E+00  1.5313909E+01
               Valence states
                 1    2    0  2.0000000E+00 -1.7424442E+00
                 2    2    1  4.0000000E+00 -6.7652133E-01
              paw valence energy after call to fcsepatom
              valence states (zvale) =  6.00000000000000000
                 1    2    0  2.0000000E+00 -1.7424449E+00
                 2    2    1  4.0000000E+00 -6.7652016E-01
              evale from sepenergyanal -3.17015915606063103E+01
             evale from matrix elements -3.17015915615520711E+01
              paw valence energy after call to fcsepatom
              valence states (zvale) =  6.00000000000000000
                 1    2    0  2.0000000E+00 -1.7424449E+00
                 2    2    1  4.0000000E+00 -6.7652016E-01
              evale from sepenergyanal -3.17015915606067935E+01
              paw valence energy after call to fcsepatom
              valence states (zvale) =  5.00000000000000000
                 1    2    0  2.0000000E+00 -2.8921118E+00
                 2    2    1  3.0000000E+00 -1.8078934E+00
              evale from sepenergyanal -3.04820270959904320E+01
```

Fig. 7. Output summary file for O projector and basis functions corresponding to "sinc", rc = 1.4 (×2) case.

```
nuclear charge     = 8
electronic charge = 8.00000000000000000
net charge         = 0.000000000000000000E+00
 .........
  calculation converged in 12 iterations
     for nz =   8
     delta(density) = 0.303518224183143697E-13
  results for loop = 12
 n l    occupancy          energy
1 0     2.0000000E+00 -3.7516303E+01
2 0     2.0000000E+00 -1.7424442E+00
2 1     4.0000000E+00 -6.7652133E-01
```

```
O                   Atom summary file name
8                   Z
2 2 0 0 0           maximum n for s, p, d, f, g shells
2 1 4               correction to maximum occupancy (n l occ)
0 0 0               end corrections
c                   core state
v                   valence state
v                   valence state
exshape             use exponential shape parameter
vloc0               allow for Vloc contribution
0                   Vloc amplitude
ipass               set remaining parameters to default values
ipass               set remaining parameters to default values
1                   lmax
1.4                 rc
n                   no new l=0 bases functions
n                   no new l=1 basis functions
O                   Atom symbol
c                   continue
2                   new valence occupancy
4                   new valence occupancy
c                   continue
2                   new valence occupancy
3                   new valence occupancy
e                   exit
```

Fig. 8. Input data for O projector and basis functions corresponding to "exp", rc = 1.4 case.

```
 Total energies
    One-electron contribution:  -81.2235788564238845
    Coulomb contribution     :   72.6579980854421876
    Exch-correl contribution :   4.94019038202986316
    Total                    :  -148.941386559836189
 for each state enter c for core or v for valence
    1  1  0   2.0000000E+00 -3.7516303E+01
>>c
    2  2  0   2.0000000E+00 -1.7424442E+00
>>v
    3  2  1   4.0000000E+00 -6.7652133E-01
>>v
 .........
 etotal = -148.941386564459066
 evale = -31.7015931876238355
 default shape function is sinc**2 and default vlocamp=0
 input "ipass" to continue or "vloc0" or "exshape"
>>ipass
 response ipass
 enter maximun 1 for basis functions
>>1
  lmax = 1
 enter rc
>>1.4
  rc 1.3999999999999991
  adjusted rc 1.4099999999999992
 iiirc,rc = 564 1.4099999999999992
```

```
           nz =  8
           Integration params -- n,rmax,small = 20000  5.0000000E+01  1.0000000E-15
             all-electron results
             core states (zcore) =  1.99999999999999334
               1    1    0  2.0000000E+00 -3.7516303E+01
             valence states (zvale) =  6.00000000000001332
               2    2    0  2.0000000E+00 -1.7424442E+00
               3    2    1  4.0000000E+00 -6.7652133E-01
             evale =  -31.7015931876238355
             paw parameters:
                shapef = exshape
                  lmax =  1
                    rc =  1.40999999999999992
                 iiirc =  564
                 gauss =  0.903788641908465973
                  kpow =  6
               vlocfac =  0.000000000000000000E+00
             Using Blochl method

           Number of basis functions      2
             No.  n   l       Energy        Cp coeff
               1    2    0 -1.7424442E+00 -1.8257615E+00
               2    2    1 -6.7652133E-01  5.0134012E+00
             Valence states
               1    2    0  2.0000000E+00 -1.7424442E+00
               2    2    1  4.0000000E+00 -6.7652133E-01
             paw valence energy after call to fcsepatom
             valence states (zvale) =  6.00000000000000000
               1    2    0  2.0000000E+00 -1.7424449E+00
               2    2    1  4.0000000E+00 -6.7652028E-01
             evale from sepenergyanal -3.17015915584259957E+01
           evale from matrix elements -3.17015900745049599E+01
             paw valence energy after call to fcsepatom
             valence states (zvale) =  6.00000000000000000
               1    2    0  2.0000000E+00 -1.7424449E+00
               2    2    1  4.0000000E+00 -6.7652028E-01
             evale from sepenergyanal -3.17015915584258039E+01
             paw valence energy after call to fcsepatom
             valence states (zvale) =  5.00000000000000000
               1    2    0  2.0000000E+00 -2.8949395E+00
               2    2    1  3.0000000E+00 -1.8106301E+00
             evale from sepenergyanal -3.04807271708155270E+01
```

Fig. 9. Output summary file for O projector and basis functions corresponding to "exp", rc = 1.4 case.

```
 .........
 Calculating basis functions using Blochl's method
   basis functions:
  No. n  l   energy   occ
   1  2  0 -1.742444E4+00  2.000000E+00
 For l = 0 there are currently 1 basis functions
 enter y to add additional functions or n to go to next l
>>y
 enter energy for generalized function
>>7
     2 999    0  7.000000E+00  0.000000E+00
 For l =  0 there are currently  2 basis functions
```

```
 enter y to add additional functions or n to go to next l
>>n
    3  2  1 -6.765213E-01  4.000000E+00
 For l = 1 there are currently  1 basis functions
 enter y to add additional functions or n to go to next l
>>y
 enter energy for generalized function
>>7
      4  999  1  7.000000E+00  0.000000E+00
For l = 1 there are currently  2 basis functions
enter y to add additional functions or n to go to next l
>>n
 completed phi basis with  4  functions
  ............

 projectors converged with loop,delta = 7 0.262620561838618066E-09
 total number of basis functions = 4
 total number of bound valence functions = 2
 error for io,l = 1 0 0.443491001301393739E-12
 error for io,l = 2 1 0.266937351129509226E-13
 calculating Fourier transforms of projector functions
 calculating Fourier transforms of smooth basis functions
 calculating Fourier transforms of tp*tphi products
 calculating logderivs for prepared basis set
 calculating log derivatives at irc 1.40000000000000013
 enter atomic symbol for atomdata file name
>>0
   8 2.0000000000000000E+00  14 ; nz,zcore,itype
  564 2.50000000000000005E-03 1.40000000000000013E+00 ; iiirc,h,rc
    4  0  0  1  1
 Calculating Fourier transform for tphilcao
  201 7.5000000E-02 ;nq,hq
 ecoul = 18.7714963667447172
        6  ; # l-diagonal matrix elements
       13  ; # l-dependent matrix elements
       73  ; # Hartree matrix elements
  atomic energy calculated for following configuration
    1    2    0 2.0000000E+00 -1.7424442E+00
    2    2    1 4.0000000E+00 -6.7652133E-01
 zvale = 6.00000000000000000
 2  0    2.0000000E+00
 2  1    4.0000000E+00

 nuclear charge   = 8
 core charge   = 1.99999999999999334
 valence electronic charge  = 6.00000000000000000
  ............
 evale from matrix elements -31.7015915615520711
evale from matrix elements -3.17015915615520711E+01
  enter c to continue or e to exit
>>c
 for each old n l occ eig listed, enter new occ
```

```
   1   2   0   2.0000000E+00 -1.7424449E+00
>>2
   2   2   1   4.0000000E+00 -6.7652016E-01
>>4
 zvale = 6.00000000000000000
 2 0      2.0000000E+00
 2 1      4.0000000E+00

 nuclear charge   =  8
 core charge  = 1.99999999999999334
 valence electronic charge = 6.00000000000000000
  ............

 total valence energy -31.7015915606067935
  enter c to continue or e to exit
>>c
 for each old n l occ eig listed, enter new occ
   1   2   0   2.0000000E+00 -1.7424449E+00
>>2
   2   2   1   4.0000000E+00 -6.7652016E-01
>>3
 zvale = 5.00000000000000000
 2 0      2.0000000E+00
 2 1      3.0000000E+00

 nuclear charge   =  8
 core charge  = 1.99999999999999334
 valence electronic charge = 5.00000000000000000
 net charge       = 1.00000000000000666
  ............
 total valence energy -30.4820270959904320
  enter c to continue or e to exit
>>e
```

5. Conclusions

We have successfully used the *atompaw* code for several different types of materials including metals, insulators, and transition metal materials. In general, we find that we must adjust the choice of the basis set and r_c^a according to the type of material and the accuracy needed for the calculation. For example, for ionic materials it may be necessary to include more upper core states in the basis set, while for elemental materials these may not be needed. In general, we iteratively check the following quantities before accepting a given set of projector and basis functions.

(1) The PAW logarithmic derivatives for each atom should agree with the all-electron values within the energy range of interest.

(2) The core electron density n_{core} should be sufficiently small for $r > r_c^a$.

(3) The plane-wave cutoffs needed to converge the calculation (which can be determined with the help of the Fourier-space functions $F_{n_i l_i}(q)$ (Eq. (25))), should be consistent with the computer resources available for the solid state calculations.

(4) For the material of interest or for a simpler material containing the same elements, a solid state calculation (using the *pwpaw* code) of the cohesive energy versus lattice constant should give a reasonable value for the equilibrium lattice constant and bulk modulus.

The authors of the *atompaw* are happy to receive feedback concerning the use of the program and the "art" of choosing PAW projector and basis parameters.

Acknowledgements

References

[1] D.R. Hamann, M. Schlüter, C. Chiang, Phys. Rev. Lett. 43 (1979) 1494–1497.
[2] G.P. Kerker, J. Phys. C: Solid St. Phys. 13 (1980) L189–L194.
[3] G.B. Bachelet, D.R. Hammann, M. Schlüter, Phys. Rev. B 26 (1988) 4199–4228.
[4] D.R. Hamann, Phys. Rev. B 40 (1989) 2980–2987.
[5] P.E. Blöchl, Phys. Rev. B 41 (1990) 5414–5416.
[6] N. Troullier, J.L. Martins, Phys. Rev. B 43 (1991) 1993–2006.
[7] D. Vanderbilt, Phys. Rev. B 41 (1990) 7892–7895.
[8] M. Fuchs, M. Scheffler, Comput. Phys. Comm. 119 (1999) 67–98.
[9] P.E. Blöchl, Phys. Rev. B 50 (1994) 17 953–17 979.
[10] N.A.W. Holzwarth, G.E. Matthews, R.B. Dunning, A.R. Tackett, Y. Zeng, Phys. Rev. B 55 (1997) 2005–2017.
[11] N.A.W. Holzwarth, G.E. Matthews, A.R. Tackett, R.B. Dunning, Phys. Rev. B 57 (1998) 11 827–11 830.
[12] G. Kresse, D. Joubert, Phys. Rev. B 59 (1999) 1758–1775.
[13] A. Tackett, N.A.W. Holzwarth, G.E. Matthews, Comput. Phys. Comm. 135 (2001) 348, this issue.
[14] W. Kohn, L.J. Sham, Phys. Rev. 140 (1965) A1133–A1138.
[15] J.P. Perdew, Y. Wang, Phys. Rev. B 45 (1992) 13 244–13 249.
[16] D.R. Hartree, The Calculation of Atomic Structures, John Wiley & Sons, Inc., 1957, pp. 85–86.
[17] M.Y. Chou, Phys. Rev. B 45 (1992) 11 465–11 468.
[18] N.A.W. Holzwarth, R.T. Williams, A. Tackett, G.E. Matthews, 2000. To be published.
[19] F.D. Murnaghan, Proc. Nat. Acad. Sci. USA 30 (1944) 244–247.
[20] X. Gonze, P. Käckell, M. Scheffler, Phys. Rev. B 41 (1990) 12 264–12 267.
[21] X. Gonze, R. Stumpf, M. Scheffler, Phys. Rev. B 44 (1991) 8503–8513.
[22] P. Blaha, K. Schwarz, J. Luitz, WIEN97, Vienna University of Technology, 1997; Improved and updated Unix version of the original copyrighted WIEN-code, which was published by P. Blaha, K. Schwarz, P. Sorantin, S.B. Trickey, Comput. Phys. Comm. 59 (1990) 399.
[23] L. Kleinman, D.M. Bylander, Phys. Rev. Lett. 48 (1982) 1425–1428.
[24] D.R. Hartree, Numerical Analysis, 2nd edn., Oxford University Press, 1958, pp. 142–143.